Implications of ballast degradation under cyclic loading

Sanjay Nimbalkar[1] and Buddhima Indraratna[2], F. ASCE

[1]Research Fellow, Centre for Geomechanics and Railway Engineering, Faculty of Engineering, University of Wollongong, Wollongong City, NSW 2522, Australia; PH (61) 2-4221-3385; FAX (61) 2-4221-3238; email: sanjayn@uow.edu.au
[2]Professor of Civil Engineering and Research Director, Centre for Geomechanics and Railway Engineering, School of Civil, Mining and Environmental Engineering, Faculty of Engineering, University of Wollongong, Wollongong City, NSW 2522, Australia; PH (61) 2-4221-3046; FAX (61) 2-4221-3238; email: indra@uow.edu.au

ABSTRACT

In spite of recent advances in track geotechnology, the understanding of the mechanisms of ballast degradation is vital for improved design to withstand high speed cyclic loading. The research conducted at Centre for Geomechanics and Railway Engineering (CGRE) at University of Wollongong (UOW) has shown that ballast degradation is influenced by various factors including the amplitude, frequency, number of load cycles, particle size distribution, confining pressure, angularity and fracture strength of individual grains. A series of cyclic drained triaxial tests were conducted using a large-scale cylindrical apparatus designed and built at UOW for frequencies ranging from 10-40 Hz. A low range of confining pressures to resemble 'in-situ' track conditions was applied. The results showed that permanent deformation and degradation of ballast increased with the frequency. Variation of the resilient modulus with respect to the degree of degradation is also discussed. Two-dimensional discrete element method (DEM) and finite element method (FEM) simulations were also carried out to capture the behaviour of ballast and the numerical results were compared with the laboratory and field data. These results quantifying the geotechnical behaviour of ballast on the micro and macro scale are described in the paper. Practical implications of these findings are discussed through field monitoring of full-scale instrumented track sections at Bulli in New South Wales.

Keywords: ballast, particle breakage, deformation, track stability, numerical models

1 INTRODUCTION

The advent and success of High Speed Railroads (HSR) in recent years has been crucial for sustainable development in passenger and freight transportation. The traditional ballast tracks are still preferred in HSR network in most countries. A ballasted rail track is categorized into two components viz. superstructure and substructure. The track superstructure consists of rail, fastening devices and sleepers. The substructure consists of ballast, subballast (capping and structural-fill) and subgrade. The ballast layer supports the track superstructure by: (i) resisting vertical, transverse and longitudinal forces from trains, (ii) distributing high stresses to protect underlying track layers and (iii) providing resiliency to absorb shock from dynamic loading. However, the ballast layer contributes the most of track settlement compared to subbalast and subgrade due to its complex behaviour under train loading (Selig and Waters 1994, Indraratna et al. 2011). The complexities associated with the ballast are attributed to the effects of angularity (Hossain et al. 2007, Sun et al. 2014), particle degradation (Indraratna et al. 2005, 2014d), in-situ confining pressure (Anderson & Fair 2008, Indraratna et al. 2010a, 2012, Altuhafi & Coop 2011), frequency of applied load cycles (Luo et al. 1996, Indraratna et al. 2011), as well as impact loads (Nimbalkar et al. 2012). The large lateral deformations of ballast due to insufficient track confinement, fouling of ballast by coal from freight trains and by clay due to pumping of soft formation soils, as well as ballast breakage, are the primary causes of track deterioration (Indraratna et al. 2013, 2014a,c, Tennakoon & Indraratna 2014).

Over many years, the design of railway tracks has focused mainly on the track superstructure often neglecting the substructure. Poor track geometry, differential settlement and large lateral displacement stems from poor performance of track substructure and inherent assumptions of available methods of design and analysis. In the past, several analytical and empirical methods have been proposed for the design of rail track (Selig & Waters 1994, Li & Selig 1998, Esveld 2001). However, these methods are based on the assumption of a homogeneous elastic half-space. Several numerical models have been developed for analysing stresses and deformations in the track (Talbot 1934, Heath et al. 1972, Chang et al. 1980, Huang et al. 1984, Dahlberg 2002). However, these studies assume elastic behaviour of track substructure, which is a serious drawback. In this paper, the salient aspects of ballast

deformations are discussed through the use of two-dimensional discrete element method (DEM) and finite element method (FEM). DEM simulations have been carried out on an assembly of irregular shaped particles. The ballast layer as a single unit is simulated in DEM while FEM analysis is performed on an integrated track model. Advanced elasto-plastic constitutive models are then implemented in FEM. Subsequently, incorporating the interaction between track components through the definition of suitable boundary conditions and load transfer mechanism, multilayered track models are simulated to capture the behaviour observed through large-scale laboratory tests and field data. This paper presents stability implications of rail track due to particle degradation under high speed cyclic loading through numerical modelling and field applications.

2 INFLUENCE OF CYCLIC LOADING IN TRIAXIAL STRESS STATE

2.1 Laboratory Testing

The influence of cyclic loading and frequency (train speed) on the deformation and degradation of ballast during cyclic loading was studied using a large-scale cyclic triaxial equipment designed and built at the University of Wollongong (Figure 1). The dynamic stresses imparted to the ballast which correspond to different frequencies were estimated in accordance with Esveld (2001). Cyclic load frequencies of 10, 20, 30 and 40 Hz were applied to simulate train speeds of 73, 145, 218 and 291 km/h, respectively (Indraratna et al., 2010c). Latite ballast was thoroughly cleaned, dried, and sieved through a set of sieves (53, 45, 37.5, 31.5, 26.5 and 19 mm). Ballast specimens were placed inside a 5 mm thick rubber membrane in four separate layers and were compacted to a density of 1530 kg/m^3. These specimens were then isotropically consolidated to a confining pressure of 60 kPa. The optimum confining pressure causing least breakage ranged from 30-90 kPa for a cyclic deviatoric stress of 500 kPa (Indraratna et al. 2005).

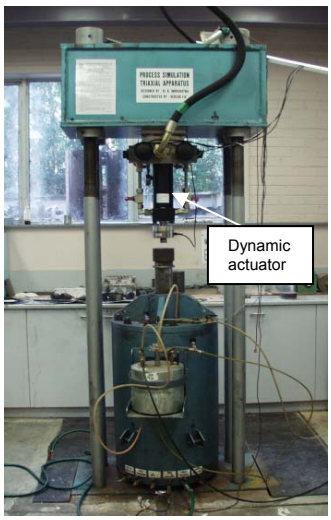

Figure 1. Cylindrical triaxial apparatus at University of Wollongong

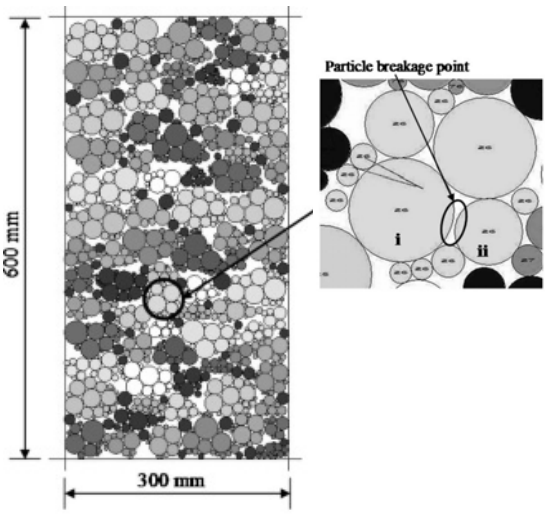

Figure 2. Discrete element model of a large-scale cylindrical triaxial test for ballast (data sourced from Indraratna et al. 2010c)

2.2 Numerical modeling using discrete element approach

In order to gain a microscopic insight into progressive failure and breakage mechanism, DEM was used. Two-dimensional numerical model was developed in DEM using PFC^{2D} (Itasca 2003) to apply a stress controlled cyclic biaxial test at the desired frequency (f) and amplitude of cyclic loading. The ballast particles were separated into different sieve sizes similar to those used during laboratory testing as described earlier. The photographs of each of the selected ballast particles were taken. These images were then filled with tangential circles and every circle was given an identification number (ID) in AutoCAD. Subroutines using built-in programming language (FISH) were developed in PFC^{2D} after gathering the ID, radius, and coordinates of the center of each circular particle representing irregular ballast particles. More details on bonding can be found in Itasca (2003). A 300 mm wide and 600 mm high biaxial cell was simulated in PFC^{2D} as shown in Figure 2. A subroutine was developed to apply a stress-controlled cyclic biaxial test at the desired frequency and amplitude of

cyclic loading. In order to save computation run time, the DEM simulations were conducted at values of N up to 1,000.

2.3 Results and discussion

Figure 3 presents the variation of accumulated permanent axial strain (ε_a) with the number of cycles (N) for different frequencies (f) of cyclic loading. A significant increase in ε_a with f was observed. For a particular value of f, ε_a rapidly increased to maximum value in the initial cycles, after which it attained a stable value at large N. This sudden increase in ε_a at low values of N could be attributed to the particle re-arrangement and breakage of asperities where high stresses had accumulated. In addition, it is evident that with an increase in f, higher values of N were required to stabilise ε_a.
The influence of f and N on particle breakage can be analysed in terms of the cumulative bond breakage (B_r) which is defined as a percentage of bonds broken compared to the total number of bonds. Figure 4 shows the variation of B_r at different f and N. It is evident that B_r increased with increase in f and N. Most of the bond breakages occurred during the initial cycles of loading, causing a higher permanent ε_a. Once the bond breakage ceased, there was an insignificant increase in ε_a. This clearly highlights that particle breakage is one of the major sources leading to permanent deformation.

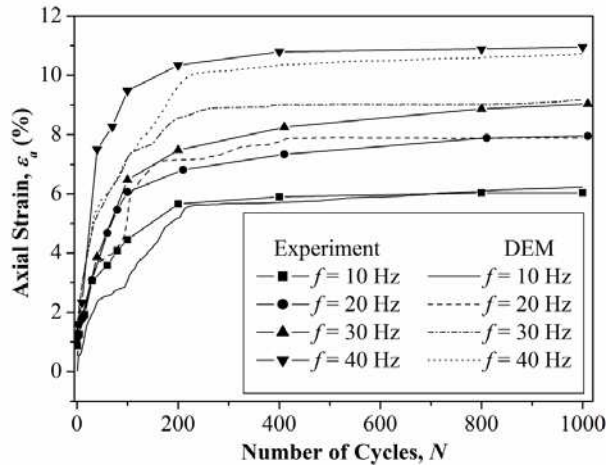

Figure 3. Comparison of axial strain (ε_a) predicted by DEM with experiment results (data sourced from Indraratna et al. 2010c)

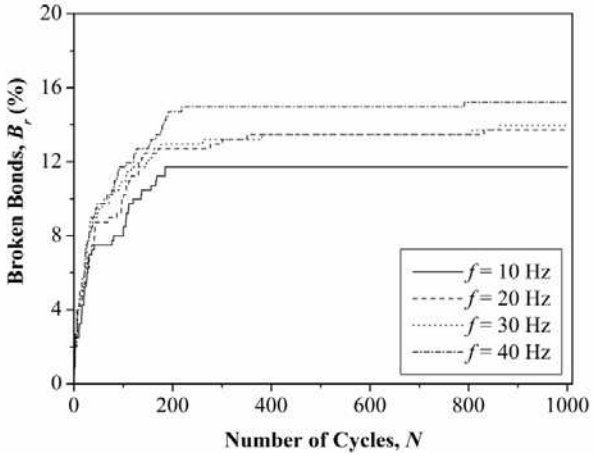

Figure 4. Effects of frequency (f) on bond breakage (B_r) with number of cycles (N) (data sourced from Indraratna et al. 2010c)

3 INFLUENCE OF CYCLIC LOADING IN THREE DIMENSIONAL STRESS STATE

3.1 Laboratory testing

A series of isotropically consolidated drained triaxial tests were conducted using the large-scale Process Simulation Apparatus (PSA) (Figure 5). PSA can accommodate a ballast specimen 800 mm in length, 600 mm in width and 600 mm in height. A cyclic load was applied by a servo-dynamic hydraulic actuator at a frequency of 15 Hz with a maximum cyclic stress of 447 kPa as per AREA method (Indraratna & Nimbalkar 2013). The hydraulic jacks mounted on the sides of the apparatus were used to provide confining pressures in two horizontal directions (perpendicular and parallel to the sleeper). The load cells connected to hydraulic jacks were used to apply the confining pressures to a prescribed range. The initial stresses were kept constant as about 7 kPa in the transverse direction (parallel to sleeper), and about 10 kPa along the longitudinal direction (perpendicular to sleeper). Numerical modeling was conducted to simulate this triaxial laboratory process and to gain more insight to the behaviour of ballast. In the following section, these numerical modeling techniques are discussed.

3.2 Numerical modeling using finite element approach

A multi-layered track model, which includes sleeper, ballast, subballast and subgrade, is simulated in a plane strain FEM using PLAXIS (version 2D 8.6, 2006) as shown in Figure 6. Elastoplastic constitutive models for ballast, subballast and subgrade are used while sleeper is simulated using

linear elastic model. An elasto-plastic hardening soil model is considered appropriate for simulating behaviour of ballast. More details on hardening soil model are given in Schanz et al. (1999). The FE model is used to capture the ballast particle degradation during the loading/reloading stage. It is assumed that only elastic deformations occur during unloading. Due to the symmetry, only half the section of model track is considered. The left and bottom boundaries are restrained in the horizontal and vertical directions, respectively, in order to simulate laboratory test conditions. The top and right boundaries are unrestrained. Small lateral pressure (σ'_3 = 7 kPa) and sinusoidal cyclic stress amplitude (σ'_{cyc}) of magnitude same as that measured during actual testing were applied to the FEM model. In order to save computation run time, the FEM simulations were conducted at values of N up to 10,000.

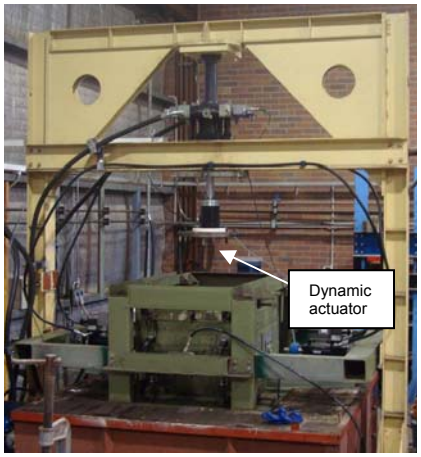

Figure 5. Process simulation testing apparatus at University of Wollongong

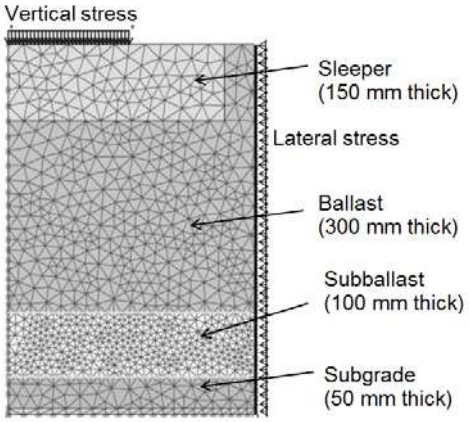

Figure 6. Finite element model of a large-scale prismoidal triaxial test for ballast (data sourced from Indraratna & Nimbalkar 2013)

The deformation of ballast is characterised by three phases. The first phase is the immediate deformation under first loading cycle. The second phase is unstable zone where the rapid deformation occurs, which is attributed to reorientation and rearrangement of particles along with significant breakage. The third phase is often termed as 'stable shakedown' during which, the rate of increase of deformation is insignificant. Thus, the ballast deformation during cyclic loading can be determined as (Indraratna & Nimbalkar 2013):

$$S_v = S_{v1}\left(1 + a\ln N + 0.5b\ln N^2\right) \quad (1)$$

where, first term refers to deformation due to first cycle, second to a unstable zone, N < 10^4 cycles, and the third term to a stable zone, N > 10^4 cycles. The long term elastic response of materials subjected to cyclic loading is often characterized in terms of the resilient modulus, M_r. In order to capture the hardening of M_r observed in triaxial tests, following equation is used (Uzan 1985):

$$E_{50}^{ref} = M_r = k_1 P_{at}\left(\frac{\theta}{P_{at}}\right)^{k_2}\left(\frac{\tau_{oct}}{P_{at}}\right)^{k_3} \quad (2)$$

where, θ is the bulk stress, τ_{oct} is the octahedral shear stress, P_{at} is the atmospheric pressure, and k_1, k_2 and k_3 are coefficients obtained by regression analysis. Equation (1) is differentiated with respect to loading cycle (N) to give:

$$\frac{d\varepsilon_v^p}{dN} = \varepsilon_{v1}^p\left(\frac{a'}{N} + \frac{b'}{N}\right) \quad (3)$$

where, ε_{v1}^p represents vertical plastic strain after the first loading cycle, and a' and b' are two empirical constants. For axi-symmetric ($\sigma'_2 = \sigma'_3$, $d\varepsilon_2^p = d\varepsilon_3^p$) and plane strain ($d\varepsilon_2^p = 0$) testing conditions, Equation (3) is expressed as (Indraratna & Nimbalkar 2013):

$$\frac{d\varepsilon_v^p}{dN} = \left(\varepsilon_{11}^p\left(\frac{a'}{N}+\frac{b'}{N}\right)\right) - \left(\frac{\sigma_1'}{\sigma_3'}\right)\left(\frac{1-\sin\phi_f'}{1+\sin\phi_f'}\right)\left(\varepsilon_{11}^p\left(\frac{a'}{N}+\frac{b'}{N}\right)\right) + \kappa\left(\frac{dBBI}{dN}\right)\left(\frac{1}{\sigma_3'}\right)\left(1-\sin\phi_f'\right) \quad (4)$$

In the above, ϕ'_f is basic friction angle of ballast and κ is an empirical coefficient (κ = 175.8). The mobilised dilatancy angle ψ_m during loading/reloading phase is expressed as:

$$\sin\psi_m = \frac{d\varepsilon_v^p}{d\varepsilon_1^p}\cdot\frac{1}{2-\frac{d\varepsilon_v^p}{d\varepsilon_1^p}} \quad (5)$$

By incorporating the effect of particle breakage in equation (5), ψ_m can be expressed as:

$$\sin\psi_m = \frac{\left[1-\left(\frac{\sigma_1'}{\sigma_3'}\right)\left(\frac{1-\sin\phi_f'}{1+\sin\phi_f'}\right)+\kappa\left(\frac{dBBI}{d\varepsilon_1^p}\right)\left(\frac{1}{\sigma_3'}\right)\left(1-\sin\phi_f'\right)\right]}{\left[1+\left(\frac{\sigma_1'}{\sigma_3'}\right)\left(\frac{1-\sin\phi_f'}{1+\sin\phi_f'}\right)-\kappa\left(\frac{dBBI}{d\varepsilon_1^p}\right)\left(\frac{1}{\sigma_3'}\right)\left(1-\sin\phi_f'\right)\right]} \quad (6)$$

It is interesting to know that the proposed modified stress-dilatancy relationship reduces to Rowe's stress-dilatancy relationship when particle breakage is ignored. Table 1 shows the material parameters used in the FE analysis. More details on the FE techniques and material parameters for other track layers are given in Indraratna & Nimbalkar (2013).

Table 1: Typical parameters used for simulation of Hardening Soil model for ballast

Parameter	Unit	Value
Confining pressure (σ'_3)	kPa	7
Secant modulus (E_{50}^{ref}) for primary stress path (=M_r)	MPa	292.7
Tangent modulus (E_{oed}^{ref}) for primary oedometer stress path (=M_r)	MPa	292.7
Stiffness modulus (E_{ur}^{ref}) for unloading-reloading stress path (=3×M_r)	MPa	878.0
Friction angle (ϕ')	degree	64.3
Dilation angle (ψ)	degree	16.4
Rate of change of BBI at failure ($dBBI/d\varepsilon_1^p$)$_f$	-	1.45

3.3 Results and discussion

The performance of ballast in this physical model subjected to cyclic loading, which represents a typical in-situ track situation, was evaluated in terms of vertical and lateral deformations. The results are summarized below. The variation of vertical (S_v) and lateral deformation (S_h) of ballast with number of loading cycles (N) is presented in Figures 7 and 8, respectively. The vertical deformation of ballast (S_v) is calculated by differentiating the vertical displacements between the sleeper-ballast and ballast-subballast interfaces, respectively. The values of vertical displacements (S_v) and lateral displacements (S_h) predicted by the FEM model showed a slight deviation from the laboratory data (Figures 7 and 8). This was possibly attributed to the fact that particle breakage was only assessed at the end of the test. Thus, 2D elasto-plastic FE analysis was able to capture the non-linear variation of S_v and S_h with number of load cycles with reasonable accuracy. The 2D (plane strain) PLAXIS analysis is adopted because the 3D analysis in PLAXIS could not accommodate cyclic loading. The experimental set up was not 2D plane strain, because the strains in the longitudinal direction could not always be maintained at zero. The comparison between the PLAXIS 2D numerical data and the experimental observations clearly elucidates this discrepancy. If a proper 3D analysis could be done with cyclic loads, then this discrepancy would be much less. The general stress condition in a three-dimensional case may affect the performance of the track system, and the current model may be potentially improved to account for this by transforming three-dimensional case into quasi two-dimensional state with adoption of appropriate boundary conditions and relevant material parameters. In the following section, FE implementation of actual track model and results are discussed.

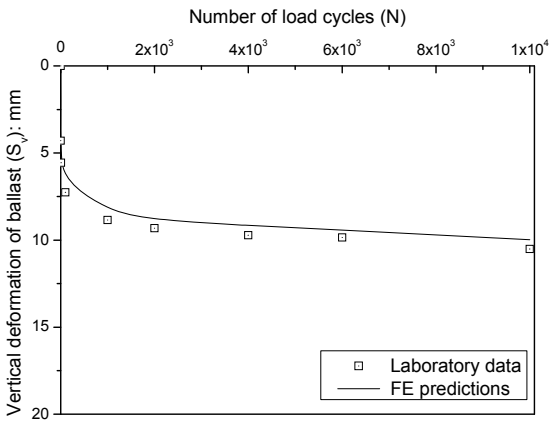

Figure 7. Variation of vertical deformation (S_v) with number of load cycles (N): FE predictions vs. test results (data sourced from Indraratna & Nimbalkar 2013)

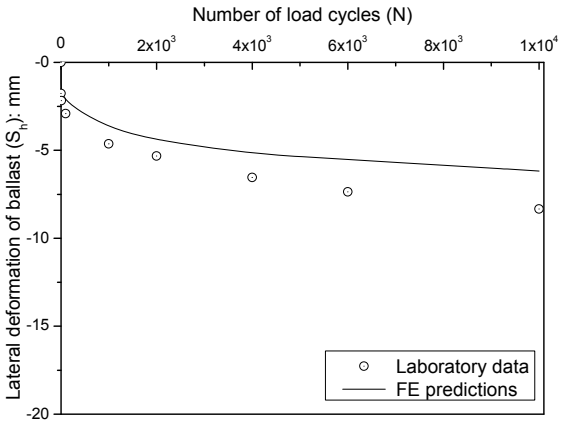

Figure 8. Variation of lateral deformation (S_h) with number of load cycles (N): FE predictions vs. test results (data sourced from Indraratna & Nimbalkar 2013)

4 FIELD TESTS ON INSTRUMENTED TRACK AT BULLI

4.1 Field investigation

In order to investigate vertical and lateral track deformations, a field trial was carried out on a real instrumented track at Bulli along the New South Coast (Figure 9). The total length of the instrumented track section was 60 m and was equally divided into four sections. The depths of ballast and subballast layer were 300 mm and 150 mm, respectively. The fresh ballast represents sharp angular coarse aggregates of crushed latite basalt. The subballast material was comprised of sand-gravel mixture. The particle size distribution of fresh ballast, subballast and other materials are given in Indraratna et al. 2010b. The performance of each section under the cyclic load of moving trains was observed by using sophisticated instruments. Vertical deformations at different sections of instrumented track were measured by settlement pegs and the lateral deformations were measured by electronic displacement transducers connected to a computer controlled data acquisition system. The settlement pegs and displacement transducers were installed beneath the rail and at the end of the sleeper at sleeper-ballast and ballast-subballast interfaces, respectively.

4.2 Numerical modeling using finite element approach

A composite multi-layered track model is simulated in a 2D plane strain FEM using PLAXIS^{2D} as shown in Figure 10. Elastoplastic constitutive models for ballast, subballast and subgrade were used while rail and sleeper were simulated as elastic materials as described in Section 2.5. In this study, 3 m high and 6 m wide plane strain finite element mesh was adopted. The nodes along the bottom boundary of the section were considered as pinned supports. The left and right boundaries were restrained in the horizontal directions, representing smooth contact vertically. The vertical dynamic wheel load was simulated as a line load representing an axle load of 25 tons with a Dynamic Amplification Factor (DAF) of 1.4, in order to incorporate the effect of train speed as traditionally used in practice (Li and Selig, 1998). The gauge length of the track was 1.68 m. The shoulder width of ballast was 0.35 m and the side slope of the railroad embankment was 1:2.

4.3 Results and discussion

In order to validate the findings of this finite element analysis, a comparison was made between the elasto-plastic analyses and the field data at the unreinforced section of track. It can be seen that the 2D FE model predicts lower values of vertical stress along the depth than those obtained in the actual field data as shown in Figure 11. One possible reason is that the real cyclic nature of wheel loading was not considered in this section and it was approximated by an equivalent dynamic loading using DAF as discussed in Section 4.2. The values of vertical displacement predicted by the elasto-plastic plane-strain analysis shows a slight deviation from the field data (Figure 12). The simulation of train wheel load as a line load and neglecting sleeper spacing may affect the stress attenuation in the

longitudinal direction of the track. Furthermore, the analysis is based on static loading rather than true dynamic repeated (cyclic) loading. These assumptions may lead to some discrepancy between the measured and predicted results. However, FE simulation of straight railway track as 2D plane strain is well established practice. Considering the limitations of the elasticity based approaches, this prediction is still acceptable for preliminary design practices.

Figure 9. Instrumented track at Bulli

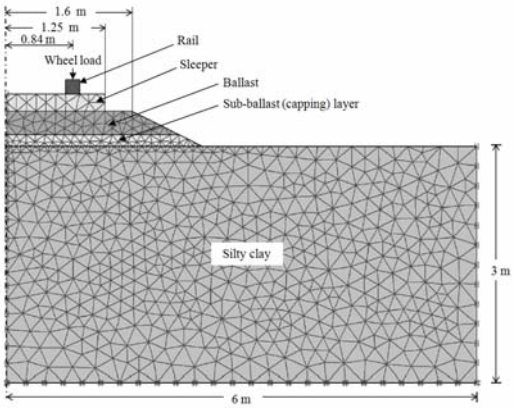

Figure 10. Finite element model of a rail track

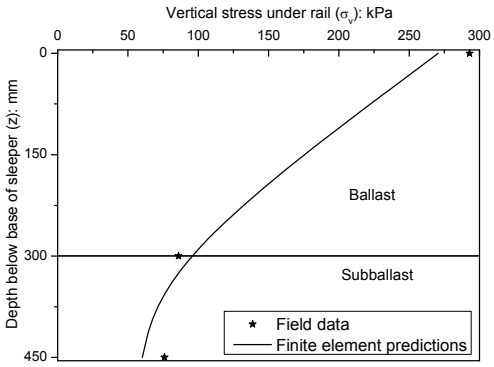

Figure 11. Vertical stresses (σ_v) under the rail: field data vs. FE predictions

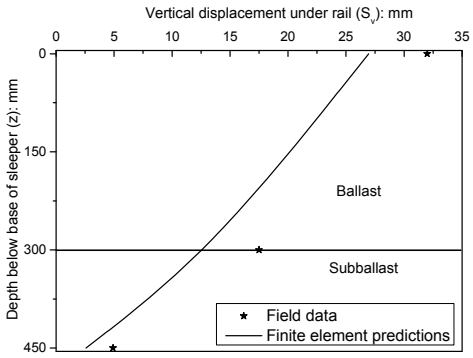

Figure 12. Vertical displacement (S_v) under the rail: field data vs. FE predictions

5 CONCLUSIONS

This paper presented the effects of particle degradation under cyclic loading on stability of ballasted rail track. Numerical simulations were performed using discrete element and finite element models. The experimental results highlighted that high frequency cyclic loading had a significant influence on the permanent deformation and degradation of ballast layer. DEM simulations captured the ballast behaviour during cyclic loading similar to the models tested in large-scale laboratory triaixial tests. The DEM based micromechanical investigation showed that most particles underwent considerable breakage during the initial stage of cyclic loading which in turn resulted into substantial axial strains. In FEM simulations, the strain-hardening behaviour of ballast was accurately simulated by using a hardening soil model. A modified flow rule could capture the effects of particle breakage and confining pressure. The results indicated that the 2D (plane strain) FEM could predict the stress-strain-degradation of both large-scale and full-scale multi-layered track model with reasonable accuracy. The advantages of the proposed DEM and FEM approaches in correctly simulating the stress-strain response of ballast were successfully demonstrated.

6 ACKNOWLEDGEMENTS

The authors wish to thank the Australian Research Council (ARC) Centre of Excellence in Geotechnical Science and Engineering and CRC for Rail Innovation. A significant portion of the contents reported here are described in more detail in a number of scholarly articles listed below. Kind permission has been obtained to reproduce some of these contents in this paper.

7 REFERENCES

Altuhafi, F., and Coop, M. R. (2011). “Changes to particle characteristics associated with the compression of sands.” Géotechnique 61 (6), 459-471.

Anderson, W. F., and Fair, P. (2008). “Behaviour of railroad ballast under monotonic and cyclic loading.” Journal of Geotechnical and Geoenvironmental Engineering ASCE 134 (3), 316-327.

Chang, C. S., Adegoke, C. W., and Selig, E. T. (1980). “GEOTRACK model for railroad track performance.” Journal of Geotechnical Engineering Division ASCE 106 (11), 1201-1218.

Dahlberg, T. (2002). “Dynamic interaction between train and nonlinear railway track model.” Proc. 5th European Conf. on Structural Dynamics, 1155-1160.

Esveld, C. (2001). “Modern Railway Track.” MRT-Productions, Netherlands.

Heath, D. L., Shenton, M. J., Sparrow, R. W., and Waters, J. M. (1972). “Design of conventional rail track foundations.” Proceedings of Institution of Civil Engineers 51, 251-267.

Hossain, Z., Indraratna, B., Darve, F., and Thakur, P. K. (2007). “DEM analysis of angular ballast breakage under cyclic loading.” Geomechanics and Geoengineering 2 (3), 175-181.

Huang, Y. H., Lin, C., Deng, X., and Rose J. (1984). “KENTRACK, a computer program for hot-mix asphalt and conventional ballast railway trackbeds.” Research Report No. RR-84-1, The Asphalt Inst. College park, Md.

Indraratna, B., Lackenby, J., and Christie, D. (2005). “Effect of confining pressure on the gradation of ballast under cyclic loading.” Geotechnique 55 (4), 325-328.

Indraratna, B., and Nimbalkar, S. (2013). “Stress-strain degradation response of railway ballast stabilized with geosynthetics.” Journal of Geotechnical and Geoenvironmental Engineering ASCE 139 (5), 684-700.

Indraratna B., Nimbalkar S., Christie D., Rujikiatkamjorn C., and Vinod J. S. (2010a). “Field assessment of the performance of a ballasted rail track with and without geosynthetics.” Journal of Geotechnical and Geoenvironmental Engineering, ASCE 136 (7), 907-917.

Indraratna, B., Nimbalkar, S., Coop, M., and Sloan, S. W. (2014a). “A constitutive model for coal-fouled ballast capturing the effects of particle degradation.” Computers and Geotechnics 61 (9), 96-107.

Indraratna, B., Nimbalkar, S., and Neville, T. (2014b). “Performance assessment of reinforced ballasted rail track.” Ground Improvement 167 (1), 24-34.

Indraratna, B., Nimbalkar, S., and Rujikiatkamjorn, C. (2014c). “From Theory to Practice in Track Geomechanics - Australian Perspective for Synthetic Inclusions.” Transportation Geotechnics Journal - Special issue on ‘Rail Geomechanics - From Theory to Practice’ doi: http://dx.doi.org/10.1016/j.trgeo.2014.07.004.

Indraratna, B., Nimbalkar, S., and Tennakoon, N. (2010b). “The behaviour of ballasted track foundations: track drainage and geosynthetic reinforcement” GeoFlorida 2010, ASCE Annual GI Conference, Florida, USA.

Indraratna, B., Thakur, P. K., and Vinod, J. S. (2010c). “Experimental and numerical Study of railway ballast behaviour under cyclic loading.” International Journal of Geomechanics, ASCE, 10 (4), 136-144.

Indraratna, B., Sun, Q. D. and Nimbalkar, S. (2014d). “Observed and predicted behaviour of rail ballast under monotonic loading capturing particle breakage.” Canadian Geotechnical Journal 10.1139/cgj-2013-0361.

Indraratna, B., Tennakoon, N., Nimbalkar, S. and Rujikiatkamjorn, C. (2013). “Behaviour of clay fouled ballast under drained triaxial testing.” Géotechnique 63 (5), 410-419.

Indraratna, B., Nimbalkar, S., and Rujikiatkamjorn, C. (2012). “Track stabilisation with geosynthetics and geodrains, and performance verification through field monitoring and numerical modeling.” International Journal of Railway Technology 1 (1), 195-219.

Indraratna, B., Salim, W., and Rujikiatkamjorn, C. (2011). “Advanced rail geotechnology - ballasted track.” CRC Press, Taylor & Francis Group, London, UK.

Itasca. (2003). “Particle flow code in two and three dimensions.” Itasca Consulting Group, Inc., Minnesota.

Li, D., and Selig, T. (1998). “Method for railroad track foundation design. I: development.” Journal of Geotechnical and Geoenvironmental Engineering, ASCE, 124 (4), 316-22.

Luo, Y., Yin, H., and Hua, C. (1996). “Dynamic response of railway ballast to the action of trains moving at different speeds.” Proceedings of the Institution of Mechanical Engineers, Part F: Journal of Rail and Rapid Transit, 210 (2), 95-101.

Nimbalkar, S., Indraratna, B., Dash, S. K., and Christie, D. (2012). “Improved performance of railway ballast under impact loads using shock mats.” Journal of Geotechnical and Geoenvironmental Engineering, ASCE, 138 (3), 281-294.

PLAXIS B. V. (2006). “PLAXIS 2D Version 8.6 - Finite element code for soil and rock analysis.” The Netherlands.

Schanz, T., Vermeer, P. A., and Bonnier, P. G. (1999). “The hardening soil model - formulation and verification.” Plaxis Symposium Beyond 2000 in Computational Geotechnics, Amsterdam Balkema, Rotterdam, 55-58.

Selig, E. T., and Waters, J. M. (1994). “Track Geotechnology and Substructure Management.” Thomas Telford, UK.

Sun, Y., Indraratna, B., and Nimbalkar, S. (2014). “Three-dimensional characterisation of particle size and shape for ballast.” Géotechnique Letters doi: http://dx.doi.org/10.1680/geolett.14.00036.

Talbot, A. N. (1934). “Stresses in railroad track-reports of the special committee on stresses in railroad track.” Seventh progress report, American Railway Engineering and Maintenance of Way Association, USA.

Tennakoon, N. and Indraratna, B. (2014). “Behaviour of clay-fouled ballast under cyclic loading.” Géotechnique 64 (6), 502-506.

Uzan, J. (1985). “Characterization of granular material.” Transportation Research Record, National Research Council, Washington, D.C. USA, 1022, 52-59.